

## Differential and total cross sections for electron-impact ionization of atomic oxygen

Tom Burnett\* and Steven P. Rountree

Department of Physics, Texas A&M University, College Station, Texas 77843

(Received 6 November 1978)

Born differential and total cross sections for electron-impact ionization of atomic oxygen are presented. A configuration-interaction wave function was used in the representation of the initial state, and a close-coupling wave function, in which the three ground-state terms of the residual ion are retained in the close-coupling expansion, was used in the description of the final state.

### I. INTRODUCTION

Electron-impact ionization is an important process in many areas of physics. In particular, ionization of atomic oxygen in the upper atmosphere affects both electron and  $O^+$  densities.<sup>1</sup>

One of the earliest attempts to estimate the total ionization cross section for atomic oxygen was made by Seaton.<sup>2</sup> He used a scaling procedure and experimental data for ionization of neon in this effort. More recently, the Born approximation has been used, in conjunction with effective-potential techniques, in the estimate of this cross section.<sup>3-5</sup> McGuire<sup>3</sup> used a Herman-Skillman potential to generate the one-electron orbitals used in the initial- and final-state representations of the target atom. Omidvar, Kyle, and Sullivan<sup>4</sup> used a screened hydrogenic orbital in the initial state, and in the final state, they used a unit-charge Coulomb function which was Schmidt orthogonalized to the bound orbital. Kazaks, Ganas, and Green (KGG)<sup>5</sup> use a potential of the form

$$V(r) = -2[(z-1)\Omega(r) + 1]/r,$$

where

$$\Omega(r) = [H(e^{r/d} - 1) + 1]^{-1}$$

and  $z$  is the nuclear charge. The two parameter,  $d$  and  $H$ , were determined by fitting the theoretical energy spectrum to the experimental ground-state ionization energy and the energy of the first 15 triplet states associated with an  $O^+(^4S^o)$  core. This potential was used in the determination of the bound and continuum orbitals.

All of these calculations are characterized by a number of approximations above and beyond the initial Born approximation. The total cross section is dominated by low-energy ejected electrons, and it is well known that independent-particle models are very crude approximations in this energy region. In the case of helium, the cross sections are typically in error by 20% or more for near-zero-energy ejected electrons.<sup>6-10</sup> With a

rather modest improvement in the initial and final states, Burnett *et al.*<sup>11</sup> obtained results which are in excellent agreement with the experimental results of Grissom *et al.*<sup>12</sup>

A great deal of work has been done on the helium-ionization problem, and in many cases, very good wave functions were used in the determination of the Born amplitudes. However, little or no work has been done on more complicated systems. Here, we report the results of a detailed calculation of a number of differential and total cross sections for ionization of atomic oxygen. Final-state interactions between the ejected electron and the residual ion, core relaxation, and correlations are very important at low ejected-electron energies and all of these effects were treated very accurately in the determination of these cross sections. In Sec. II we discuss our choice of initial- and final-state representations, and then, in Sec. III we present generalized oscillator strengths, and differential and total ionization cross sections.

### II. THEORETICAL AND COMPUTATIONAL DETAILS

The theoretical background and computational techniques are given in Ref. 13. Therefore, we give here a discussion of only those points which are pertinent to the atomic oxygen ionization problem.

A close-coupling wave function, in which the three ground-state terms of the residual ion were retained in the expansion, was used in the representation of the final state while a six-term configuration-interaction wave function was used in the representation of the initial state. The  $O^+(^4S^o)$  Hartree-Fock orbitals,<sup>14</sup> which were used in the description of the residual ion state, were augmented by an additional  $s$  and  $p$  orbital which allow for initial-state core relaxation as well as an appreciable fraction of the correlation. The near-zero momentum transfer contributions to the electron-impact

ionization cross sections are dominated by the optically allowed processes, and the agreement between the photoionization cross sections calculated in the velocity and length approximations is an excellent indication of the accuracy of the wave functions and we have employed this fact in the effort to obtain accurate representations for both the initial and final states. (The bound-state wave function is given in Ref. 15.) Our photoionization cross sections are given in Fig. 1 and are in good agreement with other works.<sup>16-21</sup> We have mapped out the lowest resonance only as a demonstration of the integrity of the computational procedures; in the determination of the electron-impact ionization cross sections we interpolated through the resonance structure.

The generalized oscillator strengths and ionization cross sections are expressed in terms of an infinite sum over bound-free reduced multipole matrix elements. We truncated the sum at a total angular momentum of  $L=6$  and an ejected-electron angular momentum  $l=4$ . Experimental energy splittings were used throughout the calculations and the noniterative integral equation method was used in the solution of the scattering equations.<sup>22</sup> The reduced matrix elements were calculated for a number of ejected-electron energies  $E$ , in the range from 0.02 to 10.0 Ry and a

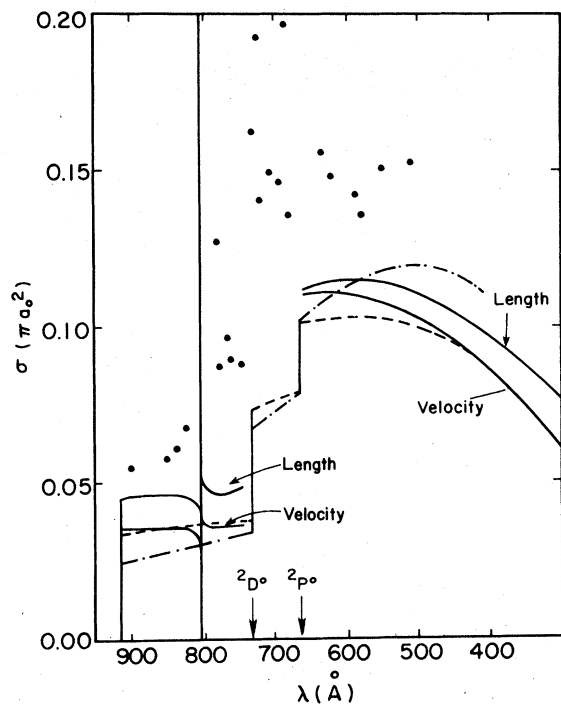


FIG. 1. Photoionization cross sections for atomic oxygen. (—) present work; (---) length results of Henry (Ref. 16); (-·-·-) velocity results of Henry (Ref. 16); (●) Cairns and Sampson (Ref. 19).

number of values of the square of the momentum transfer  $K^2$  in the range  $(0.01-10.0)a_0^{-2}$ . The coefficients in the Legendre expansion for the triple-differential cross section were computed at the grid points and spline interpolated within the grid and extrapolated to points outside of this grid. Since the major contributions to the cross sections are due to low-energy ejected electrons and values of  $K^2$  certainly less than  $10.0a_0^{-2}$ , it is clear that uncertainties in the cross sections due to small errors in the extrapolations are extremely small.

### III. RESULTS

#### A. Generalized-oscillator strengths

The generalized oscillator strengths (GOS) to the continuum are given by Eq. (21) of Ref. 13. Figure 2 shows the generalized oscillator strengths for transitions in which the residual ion final state is either  $4S^0$ ,  $2D^0$ , or  $2P^0$ . The resonance in the  $4S^0$  GOS is due to the  $4s^2D^0$  autoionizing state. The dashed portion of the curves corresponds to the GOS obtained by interpolation through the resonance structure below the  $O^+(2p^0)$ .

#### B. Double-differential cross sections

In Figs. 3 and 4 we present cross sections which are differential in the angle as well as the energy of the ejected electron. These cross sections are

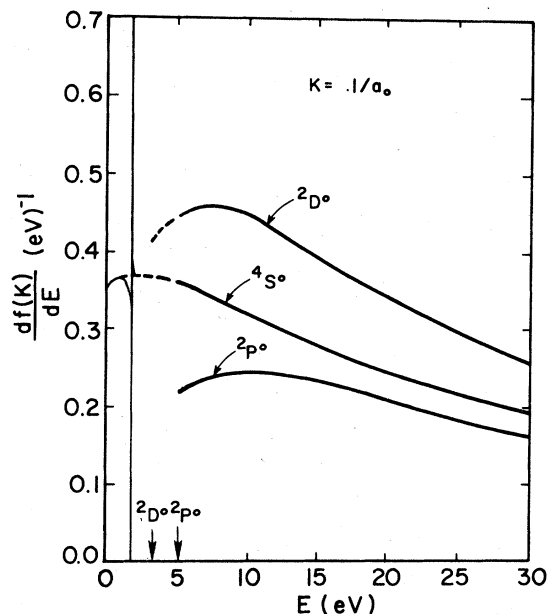


FIG. 2. Generalized oscillator strengths for the  $4S^0$ ,  $2D^0$ , and  $2P^0$  ionization channels. The dashed lines were obtained by interpolation through the resonance structure.

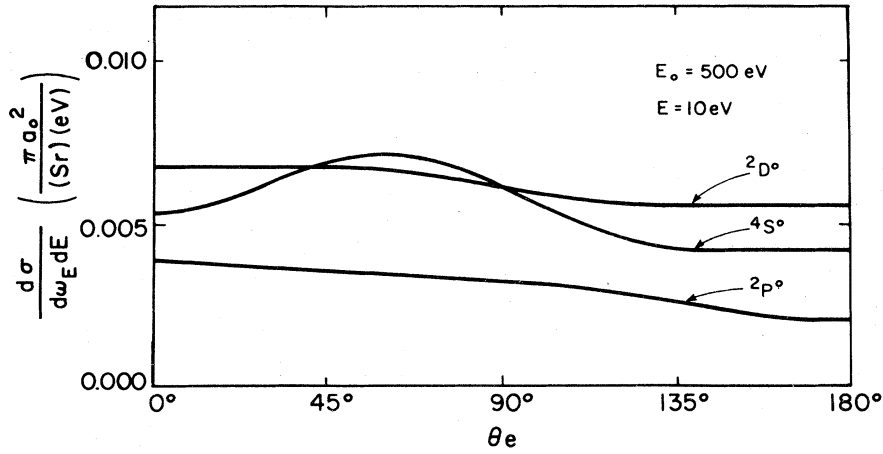


FIG. 3. Partial double-differential cross section for ejection of a  $p$ -subshell electron. The energy of the primary electron is 500 eV and the energy of the secondary electron is 10 eV. The three curves correspond to the three possible residual ion channels.

given by numerical integration of the triple-differential cross sections [see Eq. (17) of Ref. 13] over the scattering angle of the primary electron. The partial cross sections for ejection of a  $p$ -subshell electron, with a 10-eV final energy, by a primary electron of energy 500 eV are given in Fig. 3. The double-differential cross sections, summed over the residual ion states, are given in Fig. 4. The structure of the  $4S^0$  partial cross section is typical of that encountered in the ionization of helium for a primary energy greater than  $E_0 = 500$  eV; i.e., the cross sections peak between  $60^\circ$  and  $90^\circ$ . On the other hand, the  $2D^0$  and  $2P^0$  cross sections peak in the forward direction and are uncharacteristically flat. In view of the fact

that the  $2D^0$  triple-differential cross section is rather isotropic and the  $2P^0$  cross section tends to peak at about  $\pm 45^\circ$  relative to the momentum transfer axis,<sup>15</sup> the isotropy of the  $2D^0$  and  $2P^0$  double-differential cross sections is perhaps not surprising.

### C. Single-differential cross sections

The cross sections differential in the energy of the ejected electron are given by Eq. (18) of Ref. 13 and are expressed in terms of an integral over the momentum transfer. The integrand is proportional to the GOS and the partial cross sections shown in Fig. 5 clearly reflect the en-

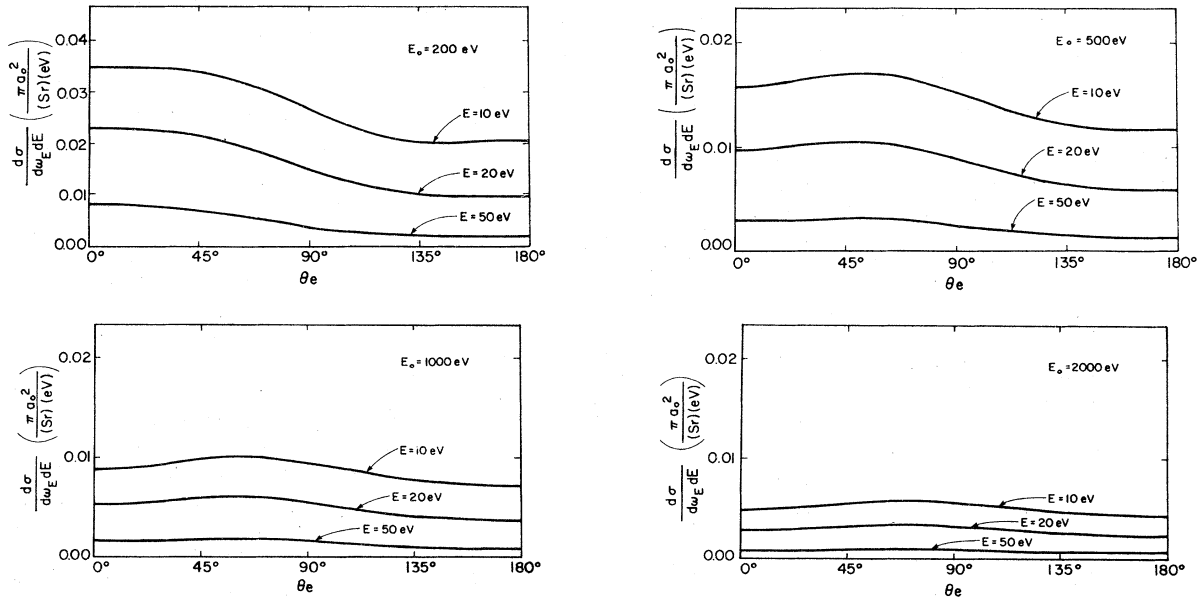


FIG. 4. Double-differential cross section for ejection of a  $p$ -subshell electron. The energies of the primary and secondary electrons are denoted by  $E_0$  and  $E$ , respectively.

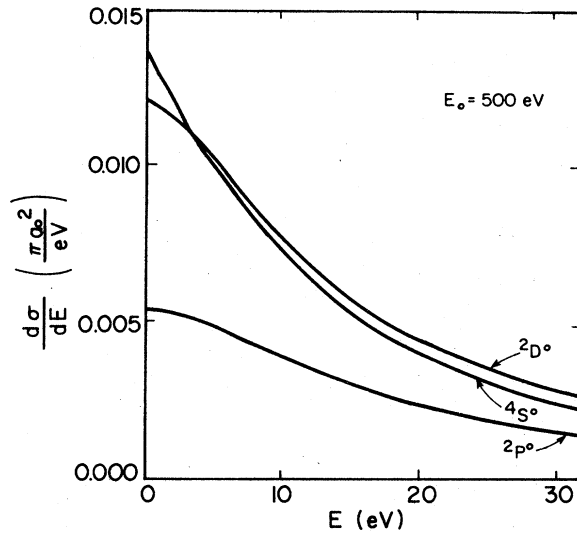


FIG. 5. Partial single-differential cross sections for ejection of a  $p$ -subshell electron. The three curves correspond to the three possible residual ion channels.

ergy dependence of the GOS's shown in Fig. 2. The cross sections for ejection of a  $p$ -subshell electron, summed over the residual ion states, are given in Fig. 6 for a number of primary-electron energies. The structure in the cross sections for ejected-electron energies of the order

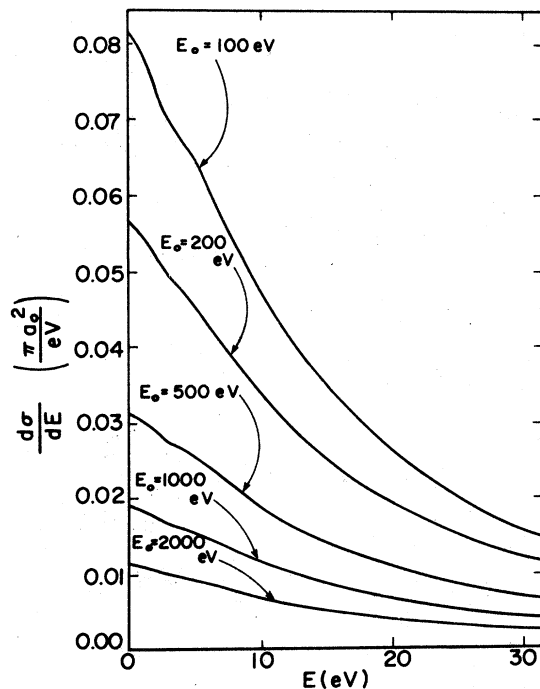


FIG. 6. Single-differential cross sections for ejection of a  $p$ -subshell electron. The energy of the primary electron is denoted by  $E_0$ .

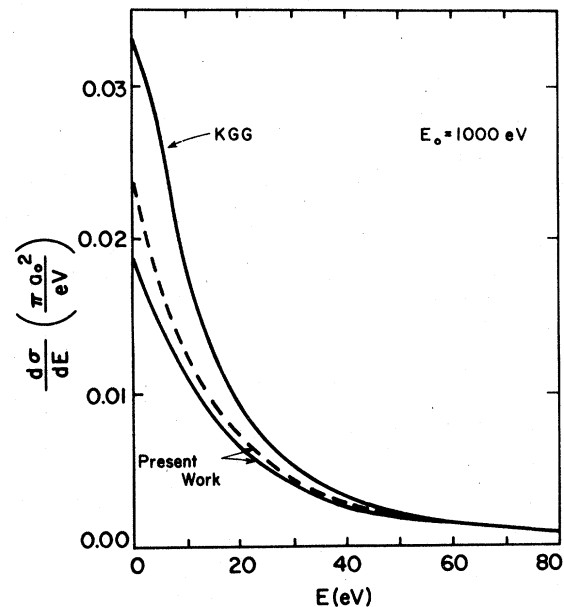


FIG. 7. Comparison of the single-differential cross sections with the results of Kazaks, Ganas, and Green (KGG).<sup>5</sup> The present results are denoted by a solid line. The  $4S^0$  partial cross section, multiplied by 3, is represented by the dashed line.

of 2 eV is due to the difference in the ejected-electron energy dependence of the partial cross sections. Figure 7 is a comparison, at an incident-electron energy of 1000 eV, of our cross sections with those of Kazaks *et. al.*<sup>5</sup> They calculated the  $4S^0$  cross section and multiplied by a factor of 3, in an effort to account for the  $2D^0$  and  $2P^0$  ionization channels. For comparison, we have multiplied the  $4S^0$  cross section by 3 and the results are indicated by the dashed curve. The KGG results are a factor of 2 greater than the present results near the ionization threshold while the agreement is much better for ejected-electron energies above 40 eV, where the atomic-structure details are much less important. This is not unexpected and is consistent with the helium ionization work.

#### D. Total cross sections

The total cross sections are given by Eq. (20) of Ref. 13. The  $4S^0$ ,  $2D^0$ , and  $2P^0$  partial contributions to the total  $p$ -subshell ionization cross section are compared with the results of Seaton<sup>2</sup> in Fig. 8. Under the circumstances, Seaton's scaling procedure gives results which agree remarkably well with the present results. The cross sections, summed over all  $K$ -shell contributions, are compared with other works in Fig. 9. The  $2s$ -subshell contributions were estimated using Seaton's scaling procedure and the  $2s$  photoionization cross

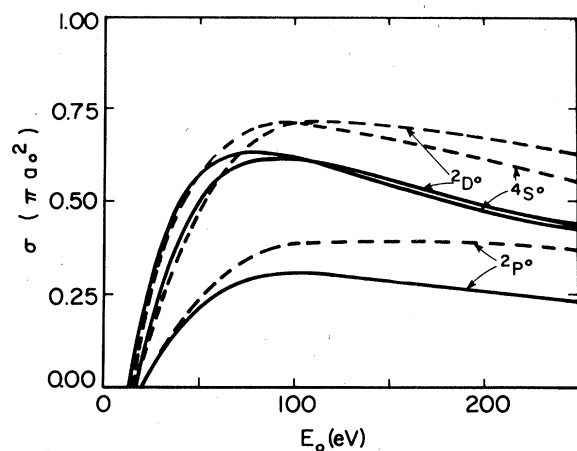


FIG. 8. Comparison of the partial contributions to the total ionization cross section with the results of Seaton.<sup>2</sup> The contributions associated with the  $4s^0$ ,  $2D^0$ , and  $2P^0$  residual ion channel are shown. —, present work; ----, Seaton.

sections of Henry.<sup>16</sup> Indications are that these contributions are less than 10% of the total cross section. The experimental results have been summarized and scrutinized by Kieffer and Dunn,<sup>23</sup> and they suggest that the cross sections measured by Boksenberg<sup>24</sup> may be too large. Fite and Brackmann<sup>25</sup> and Boksenberg<sup>24</sup> mass analyzed the ion current and therefore, they actually measured the cross section for production of  $O^+$  from  $O$  rather than the multiple ionization cross sections. All of the experimental results are normalized to the molecular oxygen ionization cross sections. Kazaks *et al.* overestimate the cross sections near the maximum and this is a reflection of the overestimate of the single-differential cross sections for low-energy ejected electrons. Otherwise, the experimental results of Fite and Brackmann,<sup>25</sup> and Rothe *et al.*,<sup>26</sup> as well as the independent-particle model calculations,<sup>3,4</sup> are in good agreement with the present results. The experimental results are in general slightly greater than the present results, but the energy dependence is in excellent agreement and perhaps, this is an indication that there is a slight error in the normalization of the experimental cross sections. However, in view of the disparity in the photoionization cross sections calculated in the velocity and length approximations, it is not clear that this is the case.

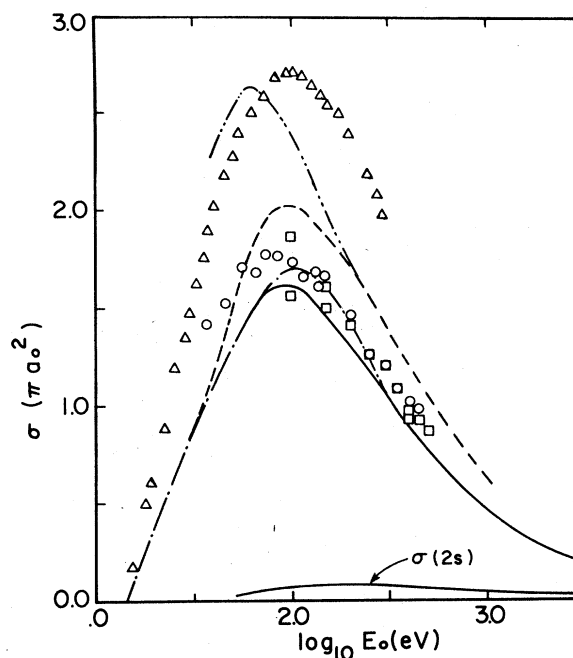


FIG. 9. Total  $K$ -shell ionization cross section for atomic oxygen. The solid curve, labeled  $\sigma(2s)$ , is our estimate of the cross section for ejection of a  $2s$  electron. The other solid curve is the present estimate for  $K$ -shell ionization; i. e.,  $\sigma(2s) + \sigma(2p)$ . Also shown on this figure are the results due to Kazaks *et al.*,<sup>5</sup> (---), Omidvar *et al.*,<sup>4</sup> (-.-.-), McGuire<sup>3</sup> (-.-.-), Boksenberg<sup>24</sup> ( $\Delta$ ), Rothe *et al.*,<sup>26</sup> ( $\square$ ), and Fite and Brackmann<sup>25</sup> ( $\circ$ ).

#### IV. CONCLUSION

Other than the work that has been done on hydrogenlike systems, there have been no previous ionization calculations in which either the initial state or the residual ion state is characterized by an open  $p$  subshell. In the present work, both states are characterized by an open  $p$  subshell and realistic wave functions have been used in the representation of both the initial and final states of the target atom.

On a more practical note, the partial cross sections are of great interest in the modeling of the ionosphere and this is the first *ab initio* calculation of these cross sections. Though there are no experimental results with which we can compare the partial cross sections, the sum over these cross sections is in very good agreement with the more reliable experimental results. Though this is encouraging, it is not sufficient to guarantee reliability of the partial cross sections.

- \*Present address: Continental Oil Co., Exploration Research Division, 102 NT, Ponca City, Okla. 74601.
- <sup>1</sup>A. D. Danilow, *Chemistry of the Ionosphere* (Plenum, New York, 1970).
- <sup>2</sup>M. J. Seaton, *Phys. Rev.* **113**, 814 (1959).
- <sup>3</sup>E. J. McGuire, *Phys. Rev. A* **3**, 267 (1971).
- <sup>4</sup>K. Omidvar, H. L. Kyle, and E. C. Sullivan, *Phys. Rev. A* **5**, 1174 (1972).
- <sup>5</sup>P. A. Kazaks, P. S. Ganas, and A. E. S. Green, *Phys. Rev. A* **6**, 2169 (1972).
- <sup>6</sup>S. T. Manson, L. H. Thoburen, D. H. Madison, and N. Stolterfoht, *Phys. Rev. A* **12**, 60 (1975).
- <sup>7</sup>V. L. Jacobs, *Phys. Rev. A* **10**, 499 (1974).
- <sup>8</sup>S. Geltman, *J. Phys. B* **7**, 1994 (1974).
- <sup>9</sup>M. Schulz, *J. Phys. B* **6**, 2580 (1973).
- <sup>10</sup>T. H. Sloan, *Proc. Phys. Soc.* **85**, 435 (1965).
- <sup>11</sup>T. Burnett, S. P. Rountree, G. Doolen, and W. D. Robb, *Phys. Rev. A* **13**, 626 (1976).
- <sup>12</sup>J. T. Grissom, R. N. Compton, and W. R. Garrett, *Phys. Rev. A* **6**, 977 (1972).
- <sup>13</sup>W. D. Robb, S. P. Rountree, and T. Burnett, *Phys. Rev. A* **11**, 1193 (1975).
- <sup>14</sup>E. Clementi, *IBM J. Res. Dev. Suppl.* **9**, 2 (1965).
- <sup>15</sup>T. Burnett and S. P. Rountree, *J. Phys. B* **11**, L1 (1978).
- <sup>16</sup>R. J. W. Henry, *Planet. Space Sci.* **15**, 1747 (1967).
- <sup>17</sup>K. T. Taylor and P. G. Burke, *J. Phys. B* **9**, L353 (1976).
- <sup>18</sup>A. K. Pradhan and H. E. Saraph, *J. Phys. B* **10**, 3365 (1977).
- <sup>19</sup>R. B. Cairns and J. A. R. Samson, *Phys. Rev.* **139**, A1403 (1965).
- <sup>20</sup>F. J. Comes, F. Speier, and A. Elzer, *Z. Naturforsch. A* **23**, 125 (1968).
- <sup>21</sup>J. L. Kohl, G. P. Lafyatis, H. P. Palenius, and W. H. Parkinson, *Phys. Rev. A* **18**, 571 (1978).
- <sup>22</sup>E. R. Smith and R. J. W. Henry, *Phys. Rev. A* **7**, 1585 (1973).
- <sup>23</sup>L. J. Kieffer and G. H. Dunn, *Rev. Mod. Phys.* **38**, 1 (1966).
- <sup>24</sup>A. Boksenberg, Thesis (University of London, 1961).
- <sup>25</sup>W. L. Fite and R. T. Brackmann, *Phys. Rev.* **113**, 815 (1959).
- <sup>26</sup>E. W. Rothe, L. L. Marino, R. H. Neynaber, and S. M. Tryjillo, *Phys. Rev.* **125**, 582 (1962).